JACS Au
AN OPEN ACCESS JOURNAL OF THE AMERICAN CHEMICAL SOCIETY

pubs.acs.org/jacsau
Article

Kinetic and Mechanistic Studies of Native Chemical Ligation with Phenyl α-Selenoester Peptides

Iván Sánchez-Campillo and Juan B. Blanco-Canosa*

Cite This: JACS Au 2024, 4, 4374−4382
Read Online

ACCESS | Metrics & More | Article Recommendations | Supporting Information

ABSTRACT: Native chemical ligation (NCL) ligates two unprotected peptides in an aqueous buffer. One of the fragments features a C-terminal α-thioester functional group, and the second bears an N-terminal cysteine. The reaction mechanism depicts two steps: an intermolecular thiol−thioester exchange resulting in a transient thioester, followed by an intramolecular *S-to-N* acyl shift to yield the final native peptide bond. Although this mechanism is well established, the direct observation of the transient thioester has been elusive because the fast intramolecular rearrangement prevents its accumulation. Here, the use of α-selenoester peptides allows a faster first reaction and an early buildup of the intermediate, enabling its quantification and the kinetic monitoring of the first and second steps. The results show a correlation between the steric hindrance in the α-thioester residue and the rearrangement rate. In bulky residues, the *S-to-N* acyl shift has a significant contribution to the overall reaction rate. This is particularly notable for valine and likely for other similar β-branched amino acids.

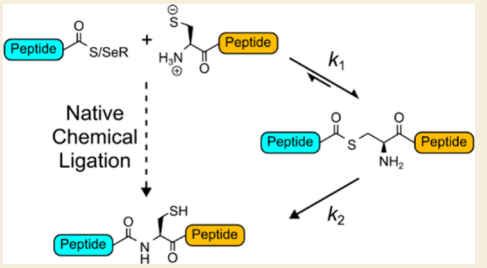

KEYWORDS: *Native chemical ligation, Thioesters, Selenoesters, Peptides, Chemical protein synthesis*

INTRODUCTION

NCL forms naturally occurring peptide bonds via the condensation of unprotected peptides.[1,2] It is a paramount reaction in synthetic protein chemistry and has allowed the preparation of hundreds of proteins.[3,4] The mechanism involves a two-step bimolecular reaction (Scheme 1): first (step 1), a reversible intermolecular transthioesterification between a peptide containing a C-terminal alkyl or phenyl α-thioester (**A**, donor peptide), and the thiolate moiety of a second fragment bearing an N-terminal cysteine (**B**, acceptor peptide). This condensation yields a transient thioester (**AB**). Following the acyl-donor capture, the second step comprises an intramolecular nucleophilic attack of the α-amine to the thioester and concurrent displacement of the thiol to give the final amide bond (**P**, product).[1,2,5,6] The *S-to-N* acyl rearrangement is the driving force pushing the equilibrium toward the product (step 2).

NCL is typically carried out under mild aqueous conditions, i.e., pH = 7.0 and room temperature. At neutral pH, the N-terminal thiolate possesses a higher nucleophilicity, and the attack to the α-thioester is faster, although its concentration compared to other functional groups (hydroxyls, imidazoles, carboxylates, and protonated amines) is lower. Moreover, the addition of different chaotropic and denaturing agents (guanidine hydrochloride = Gdm.HCl, urea) to the ligation buffer enhances peptide solubility and improves the ligation kinetics. The ligation rate strongly depends on the nature of the thiol-leaving group, and the C-terminal residue of the α-thioester fragment: phenyl α-thioesters are more reactive than

Scheme 1. Mechanism of the NCL

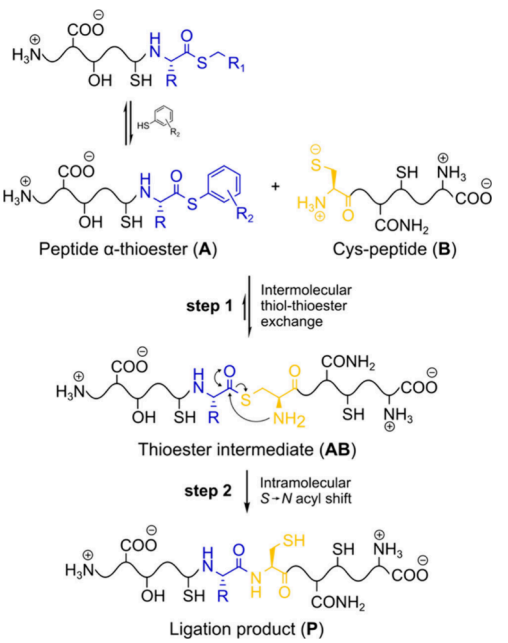

Received: August 5, 2024
Revised: October 14, 2024
Accepted: October 14, 2024
Published: October 30, 2024

alkyl, and bulky residues slow down the ligation rate, very noticeable in the case of Val and Ile.[7] The **A** peptide also undergoes the attack of other thiolates present either in **A**, **B**, and **P**, resulting in cyclic or branched thioesters.

These are less reactive, but the addition of exogenous thiols (commonly phenyl thiols with a pK_a ∼ 6.5−7.0) reverses these unproductive peptides by forming highly activated phenyl α-thioesters. Therefore, in the traditional NCL approach, C-terminal alkyl α-thioester peptides and Cys-peptides **B** are incubated in the presence of phenyl thiols (100 - 200 mM). These phenyl thiols catalyze the thiol-thioester exchange and increase the ligation rate.[7−9]

The original NCL concept has been extensively studied, and alternative methods to Boc-chemistry for α-thioester synthesis plus other ligation sites distinct from N-terminal Cys have been established. These developments were encouraged by the prominent use of Fmoc-SPPS and the challenging preparation of α-thioester peptides. The discovery of thioester surrogates enables peptide thioesterification by exchange with thiols and, in some of these approaches, concomitant NCL.[3,10] On the other side, the scarcity of Cys residues in proteins (1.5%) prompted the search of other ligation sites, with Ala and Gly-derived N-auxiliaries attracting most of the attention due to their high abundance in proteins (Ala 8.7%, Gly 6.8%): Ala can be replaced by Cys[11] or selenocysteine[12,13] and reduced to Ala after ligation using chemoselective methods.[11,14,15] Similarly, Gly N-auxiliaries rely on thiol (or selenol) scaffolds attached to the α-amino group of Gly. Upon transthioesterification with **A**, they undergo 5- or 6-membered ring transition state rearrangement in an NCL-type reaction.[16−19] The final detachment of the N-auxiliary yields the native peptide backbone. Other approaches require the stereospecific installation of sulfhydryl (or selenol) groups on the β- or γ- positions of a particular amino acid.[20,21] However, these strategies are not highly extended due to the complex synthesis of the building blocks.

Mechanistically, the analysis of the reaction pathway assumes an equilibrium shifted toward the α-thioester **AB** and a spontaneous intramolecular rearrangement.[1,2,6,8,9] Indeed, **AB** has only been observed under nondenaturing and template NCL conditions, reinforcing the hypothesis of the thiol-thioester exchange as the rate-limiting step.[22] Therefore, a second-order reaction (**A** + **B** → **P**) represents the two-step mechanism. The equation usually includes the previous rate-limiting phenyl thiol-alkyl thioester exchange, as well. This simplification has derived into a wide knowledge of the transthioesterification phase, enabling the design of better thiol catalysts, but also precluding studies about the intramolecular *S-to-N* acyl shift and its contribution to the reaction rate. Moreover, this lack of experimental data has restricted our understanding of the stereoelectronic effects controlling the slow kinetics observed for Val, Ile, and Pro. Recently, C-terminal α-selenoesters ($\mathbf{A_{Se}}$) have imprinted a new vision of NCL thanks to rate enhancements of 10-fold over the analogous phenyl α-thioester NCL.[23,24] For instance, the reaction time in Pro is reduced from > 1 day to around 2 h.[23] This rate increment results from an acceleration of the first step because **AB** stays unchanged independently of the initial peptide donor.

In this work, we have used preformed phenyl α-selenoesters to characterize the *S*-acyl intermediate and determine the kinetics of both steps. The ligations were carried out using model $\mathbf{A_{Se}}$ sequences (LYRAXaa-COSePh, Xaa = Ala, Val, and Pro), and **B** peptides: CTAFS, (hCys)TAFS (hCys = homocysteine), (MeCys)TAFS (MeCys = N-methylcysteine). These prototypical peptides are readily synthesized and the ligations are monitored by LC-MS.[7−9] The $\mathbf{A_{Se}}$ C-terminal residues intend to represent the range of kinetics of the twenty proteogenic amino acids, mainly accounting for the reactivity due to stereoelectronic effects. The **B** N-terminal amino acids MeCys and hCys mimic systems undergoing rearrangement through 5 and 6-membered ring transition states including N-auxiliaries. We have also compared the reactivity of phenyl α-selenoesters and phenyl α-thioesters using the peptide LYRAV-COS(4-MBA) (4-MBA = 4-mercaptobenzoic acid). As expected, phenyl α-selenoesters react faster, although a strict comparison would require a thiol-leaving group with a similar pK_a to PhSeH.

RESULTS AND DISCUSSION

NCL with C-Terminal Val-SePh

In our previous communication, we identified a compound during the first seconds of the NCL between LYRAF-COSePh and CTAFS. This peptide evolved to the ligated product (LYRAFCTAFS) and had the same *m*/*z*.[25] We anticipated the configuration of this compound as the searched peptide **AB**. Therefore, we continued our investigations to elucidate its structure and reactivity in the context of a broader project launched to calculate the rate constants of different phenyl α-thioester and phenyl α-selenoester peptides. Thus, LYRAV-COSePh was selected anticipating a kinetic profile between Pro and Ala. Liquid chromatography analysis afforded the concentration of the different ligation products at the selected times using Tyr (2.0 mM) as an internal standard reference.

LYRAV-COSePh (**1**, 1.7 mM) and CTAFS (**2**, 2.6 mM) were incubated at pH = 6.9 and 23 °C (Scheme 2), in an aqueous

Scheme 2. NCL between Peptides 1 and 2

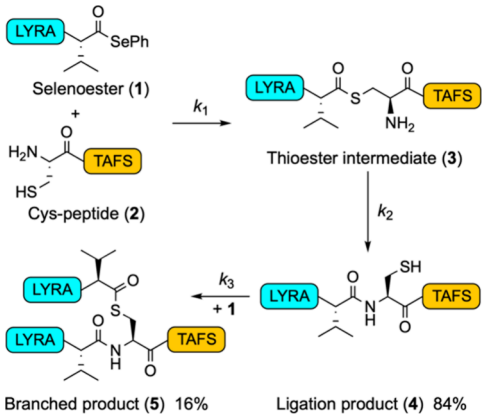

phosphate buffer (5.0 M Gdm, 0.17 M sodium phosphate) containing diphenyl diselenide (DPDS, 50 mM), and the reducing agent tris(2-carboxyethyl)phosphine (TCEP, 100 mM). Aliquots of the ligation were withdrawn at specific times and quenched by acidification with the same volume of $HCl_{(aq)}$ (0.5 M). The first 10 min of the ligation showed the coincidence of two products with identical *m*/*z* (**3** and **4**, *m*/*z* 1129.7, Figure 1). Following the formation and disappearance of **3**, the expected product (**4**, 84%) and the branched LYRAVC-(LYRAV[COS-])TAFS thioester (**5**, 16%) grew until the consumption of **1**.

Therefore, **3** likely represented the *S*-acyl thioester intermediate, as described in the mechanism of NCL. Then, we scaled up the reaction to characterize **3** by ^{13}C NMR (Figure

https://doi.org/10.1021/jacsau.4c00705
JACS Au 2024, 4, 4374−4382

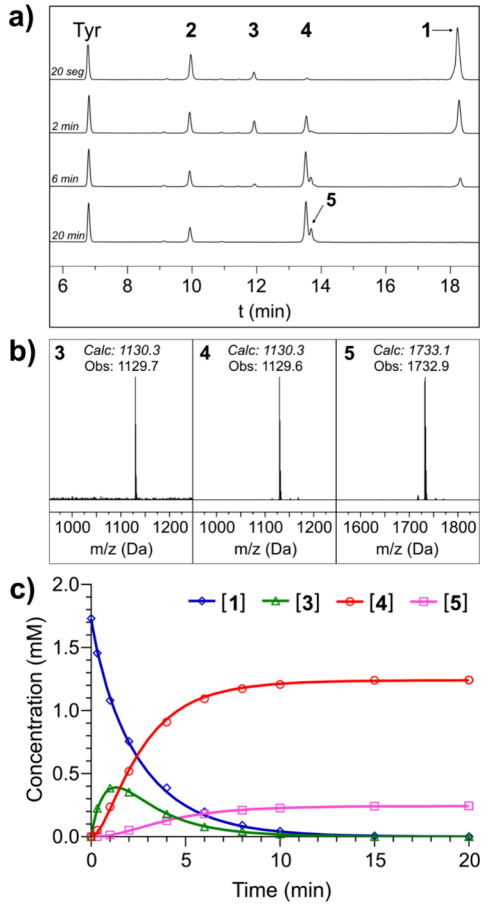

Figure 1. (a) Representative HPLC traces at 220 nm of the NCL between **1** and **2**; (b) MALDI-TOF MS of peptides **3**, **4**, and **5**; (c) experimental data (dots) and their corresponding curve fitting (solid lines) using the model **1** + **2** → **3** → **4** + **1** → **5**.

2): **1*** (6.50 mg, 5.80 × 10^{-3} mmol, ^{13}C-labeled at the Val carbonyl) and 5 equivalents of **2** (18.9 mg, 2.96 × 10^{-2} mmol) were mixed in an aqueous phosphate buffer (pH = 7.0, 2.5 mL). The use of an excess of **2** boosted the initial intermolecular reaction and also minimized the formation of branched thioesters. The reaction was quenched after 45 s with an equal

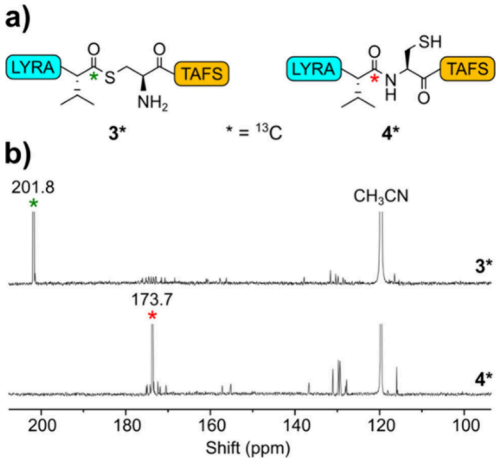

Figure 2. (a) Chemical structures of peptides **3*** and **4***; (b) ^{13}C NMR (126 MHz) spectra of **3*** and **4*** in a mixture of CH_3CN (not deuterated):D_2O (10:90) containing [DCl] = 5.0 mM.

volume of $HCl_{(aq)}$, yielding a mixture of **3***:**4*** (1.2:1 by HPLC) plus unreacted **1*** (Figure S24). **3*** (2.20 mg, 24%) was recovered following HPLC purification and lyophilization. Peptide **3*** was stable at pH < 2 but rearranged to **4*** upon increasing the pH. Importantly, ^{13}C NMR of **3*** in acidic deuterated water showed a signal at 201.8 ppm characteristic of a thioester group (Figure 2). Conversely, in the peptide **4*** the signal appears at 173.7 ppm, distinctive of an amide bond. In conclusion, we confirmed the structure of peptide **3*** as the *S*-acyl α-thioester intermediate described in the mechanism of NCL. Further experiments in the presence of H_2NOH (5 M, pH = 6.0) partially trapped **3***, resulting in the formation of the LYRAV*-CONHOH peptide (Figures S28 and S29).

The mechanism of NCL (Scheme 1) hypothesizes an equilibrium between **AB** and the α-thioester species **A**. Nevertheless, phenylselenol or common phenyl thiols (4-MPOH = 4-mercaptophenol, 4-MPAA = 4-mercaptophenyl acetic acid) used in NCL do not shift the equilibrium toward the α-thioester form because $k_1 \gg k_{-1}$. Thus, the kinetic analysis is simplified and the system is analyzed as consecutive steps of irreversible reactions:

$$\mathbf{A} + \mathbf{B} \rightarrow \mathbf{AB}\ (k_1) \quad (1)$$

$$\mathbf{AB} \rightarrow \mathbf{P}\ (k_2) \quad (2)$$

$$\mathbf{P} + \mathbf{A} \rightarrow \mathbf{PA}\ (k_3) \quad (3)$$

Where equation 3 represents the reaction for the formation of the branched product (**PA**). Assuming these postulates, full reaction profiles of **AB**, **P**, and **PA** (**3**, **4**, and **5**, respectively in Figure 1) were examined to calculate the corresponding kinetic constants (k_1, k_2, and k_3) using simulations of elementary unimolecular and bimolecular reaction steps (Figure 1c).[26] The results, obtained from triplicate experiments, were (Table 1, entry 1): k_1 = (3.2 ± 0.1) $M^{-1}s^{-1}$, k_2 = (0.0160 ± 0.0009) s^{-1} ($t_{1/2}$ = 43 s), k_3 = (1.9 ± 0.1) $M^{-1}s^{-1}$. We measured independently the rates for transformations: **3** → **4** and **1** + **4** → **5**, obtaining values of k_2 and k_3 similar to the numbers calculated with the three-step state model (Table 1, entries 2 and 3). Moreover, NCL between **1** (1.4 − 1.7 mM) and **2** (8.3 mM) carried out in the same ligation buffer (5.0 M Gdm, 0.17 M sodium phosphate, 50 mM TCEP, pH = 6.9 − 7.0), but devoid of phenylselenol (originated from the in situ reduction of DPDS) provided equivalent rate constants: k_1 = (3.7 ± 0.2) $M^{-1}s^{-1}$, k_2 = (0.0132 ± 0.0003) s^{-1}, indicating the nonexistence of catalytic effect on the kinetics of these preformed phenyl α-selenoesters (Figures S36, S37, and S38 and Table S3).

The kinetic model predicts very accurately the distributions of the different products: **3** reaches its maximum concentration around 75 s (0.38 mM) in a ratio **3**:**4** of 1.2:1. But while the [**3**] just hit its peak, the [**4**] experiences a fast growth until the first ~ 5 min (83% of the total product). Interestingly, k_3 is in the same order of magnitude as k_1 (only 0.6-fold smaller), thus explaining the fast generation of **5**. The model foresees the use of a 5-fold excess of **2** to decrease the ratio of the branched product **5** to less than 3%, as experimentally observed (Figures S36, S37, and S38) and previously reported.[23] When the system was adjusted to a model: **A** + **B** → **P** + **A** → **PA**, the obtained k_{obs} (k_{12}) = (2.0 ± 0.1) $M^{-1}s^{-1}$ was smaller than k_1 and did not describe well the system: it overestimated during the first 4 min 30 s the amount of product because presumed its appearance from the onset of the ligation, obviating the generation of **AB** (Figure S35).

https://doi.org/10.1021/jacsau.4c00705
JACS Au 2024, 4, 4374−4382

Table 1. Kinetic Constant Parameters for the NCL with Model Peptides[a]

Entry	Donor (A/A_{Se})	Acceptor (B, AB, P)	k_1 (M^{-1} s^{-1})	k_1 ratio	k_2 (s^{-1})	$t_{1/2}$ (AB, s)[b]	k_3 (M^{-1} s^{-1})	k_{-3} (M^{-1} s^{-1})
1[c]	**1**	**2**	3.2 ± 0.1	1	0.0160 ± 0.0009	43	1.9 ± 0.1	n.d.
2		**3**			0.018 ± 0.001	39		
3[d]	**1**	**4**					2.1 ± 0.2	n.d.
4[d]	**1**	**7**	0.45 ± 0.02	0.14	0.0016 ± 0.0002	433	n.d.	n.d.
5[d]	**1**	**11**	5.5 ± 0.4	1.7	0.0012 ± 0.0002	577	n.d.	n.d.
6[e]	**6**	**2**	0.23 ± 0.01	0.072	0.019 ± 0.004	36	0.11 ± 0.02	0.0010 ± 0.0003
7[e]	**6**	**4**					0.13 ± 0.04	0.0011 ± 0.0005
8[f]	**14**	**2**	26 ± 2	8.1	0.22 ± 0.01	3	n.d.	n.d.
9[c]	**18**	**2**	0.72 ± 0.03	0.23	0.031 ± 0.001	22	n.d.	n.d.

[a]**1**: LYRAV-COSePh, **2**: CTAFS, **3**: LYRAV([COS-])CTAFS, **4**: LYRAVCTAFS, **6**: LYRAV-COS(4-MBA), **7**: (hCys)TAFS, **11**: (MeCys)TAFS, **14**: LYRAA-COSePh, **18**: LYRAP-COSePh. Buffer composition: [Gdm] = 5.0 M, [sodium phosphate] = 0.17 M, [Tyr] = 2.0 mM, pH = 6.9−7.0, 23 °C. [b]$t_{1/2} = \ln(2)/k_2$. [c][DPDS] = 50 mM, [TCEP] = 100 mM. [d][DPDS] = 20 mM, [TCEP] = 50 mM, [ascorbate] = 0.2 M. [e][4-MBA] = 100 mM, [TCEP] = 50 mM. [f][TCEP] = 50 mM.

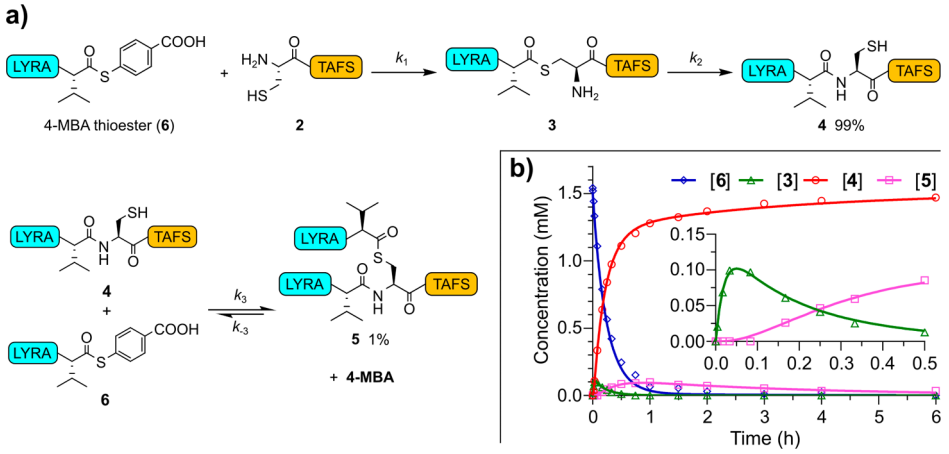

Figure 3. (a) NCL between peptides **6** and **2**; (b) experimental data (dots) and their corresponding curve fitting (solid lines) using the model **6** + **2** → **3** → **4** + **6** ⇌ **5** + 4-MBA.

Although from these experiments the rate-limiting step could not be determined due to the different order of the kinetic constants, the half-life of **3** (43 s) and the first half-life of **1** (96 s) point out that the transthioesterification has the slowest rate, also visible observing the disappearance curves of **1** and **3** (Figure 1c). Simulations using the computed constants, a $[\mathbf{1}]_o$ = 1.7 mM, and a $[\mathbf{2}]_o$ = 3.7 mM show an overlapping in the disappearance curves of **1** and **3** after the first 4 min 30 s of reaction, indicating a balance in the rate of both steps (Figure S34). Concentrations of **2** > 3.7 mM promote a faster first step resulting in a larger accumulation of **3**, as is observed when the $[\mathbf{2}]_o$ is 5-fold over the $[\mathbf{1}]_o$ (Figure S37).

NCL with C-Terminal Val-(4-MBA)

The next question was to figure out if **AB** could be detected using α-thioesters. Therefore, we prepared a phenyl α-thioester peptide with a good leaving group to increase the rate of the transthioesterification step: LYRAV-COS(4-MBA) (**6**, 4-MBA = 4-mercaptobenzoic acid with a pK_a of 4-MBA = 5.5).[27] Using typical NCL conditions for phenyl thiol ligations ([4-MBA] = 100 mM, [TCEP] = 50 mM, pH = 7.0, 23 °C), a $[\mathbf{6}]_o$ = 1.8 mM, and a $[\mathbf{2}]_o$ = 3.3 mM (Figure S44 and S45), it was possible to detect **3** although its maximum concentration (0.054 mM at 150 s) only represented a 3% of the final product **4**, 10-fold lower compared to the α-selenoester ligation.

Increasing 2-fold the number of equivalents of **2** ($[\mathbf{6}]_o$ = 1.5 mM, $[\mathbf{2}]_o$ = 5.2 mM), **3** doubled its highest concentration at 180 s (Figure 3). This implied a low accumulation of **3**. Applying the same kinetic model as in the ligation with **1**, but this time considering the equilibrium: **P** + **A** ⇌ **PA** + 4-MBA (**4** + **6** ⇌ **5** + 4-MBA), it was obtained a k_1 = (0.23 ± 0.01) $M^{-1}s^{-1}$ that is 14-fold smaller than the corresponding k_1 for the α-selenoester ligation (Table 1, entry 6). The disappearance curves of **6** and **3** reflect a slower first phase. To make the first reaction faster, the concentration of **2** needs to be at least 28-fold higher when the $[\mathbf{6}]_o$ = 1.5 mM (Figure S46).

The NCL with **6** revealed the equilibrium between **4**, **5**, **6**, and 4-MBA. During the ligation with the phenyl α-selenoester, the formation of **5** was irreversible due to the slow rate of phenylselenol-(α-thioester) exchange. The corresponding rate constants and the initial concentration of reactants determined the final distribution of products at the end of the reaction. However, 4-MBA promoted the transthioesterification of the 4-MBA thioester, pushing the equilibrium to the amide product **4** until the termination of the cycle, giving a final ratio of 99:1 (**4**:**5**) after 6 h. The slow disappearance of the branched peptide suggested **5** as the main species in the equilibrium. Corroborating this hypothesis, when **4** (1.3 mM) and **6** (4.4 mM) were incubated in the presence of 4-MBA (100 mM), the system reached the equilibrium after 150 min giving a ratio **5**:**4** of 8:2 (Figure 4). The calculated constants were (Table 1, entry 7): k_3 = (0.13 ± 0.04) $M^{-1}s^{-1}$, k_{-3} = (0.0011 ± 0.0005) $M^{-1}s^{-1}$, K_{eq} = 123 ± 20 (Table S7). Therefore, the forward reaction is faster than the reverse, determining the slow growth of **4** after

https://doi.org/10.1021/jacsau.4c00705
JACS Au 2024, 4, 4374−4382

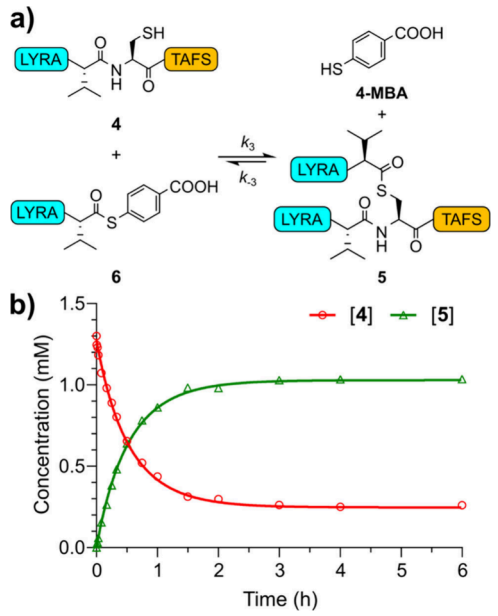

Figure 4. (a) Transthioesterification equilibrium between peptides **4**, **5**, and **6**; (b) experimental data (dots) and their corresponding curve fitting (solid lines) using the model **4** + **6** ⇌ **5** + 4-MBA.

the first ∼ 50 min, where the highest [**5**] was achieved (Figure 3b).

The branching constant k_3 is only 0.6-fold smaller than k_1, meaning a direct competition for the acyl-4-MBA donor. Other combinations of acyl donors and thiols, such as those derived from 4-MPAA and 4-MPOH, should have lower k_3 and larger k_{-3} due to their higher pK_a (pK_a 4-MBA = 5.5 versus pK_a 4-MPAA = 6.6).[9] As a consequence, they will be poorer leaving groups than 4-MBA but better nucleophiles, and the overall observed rates for the catalysis with α-alkyl thioesters will be faster.

NCL of C-Terminal Val-SePh with N-Terminal hCys and MeCys

In NCL the low abundance of Cys represents a problem in protein synthesis when the residue is not properly positioned. Hence, the search for other ligation sites becomes necessary and N-auxiliaries represent an alternative. Thus, it would be useful to compare the rearrangement rates of 5 and 6-membered rings including hCys, and N-alkylated Cys (MeCys and MehCys, MehCys = N-methylhomocysteine, Figure 5). To figure out this, we prepared the peptides (hCys)TAFS (**7**), (MeCys)TAFS (**11**), and (MehCys)TAFS. hCys is a precursor for Met junctions,[28,29] while MeCys and MehCys depict simplified models of N-auxiliaries rearranging through 5 and 6-transition state membered rings.

NCL between **1** (1.3 mM) and **7** (5.1 mM) showed a decrease in the rate of both steps, resulting in a longer disappearance time of the intermediate thioester **8** to yield the product **9** (91%) and the branched thioester **10** (2%) (Figures 5a,b). The calculated constants were (Table 1, entry 4): k_1 = (0.45 ± 0.02) $M^{-1}s^{-1}$ and k_2 = (0.0016 ± 0.0002) s^{-1} ($t_{1/2}$ = 433 s), 7 and 10-fold smaller than the respective values obtained with **2**. The decrease in k_1 is likely due to the low population of the thiolate species present in the solution: at pH 7.0 the concentration of available thiolate is less than 0.5% (estimating a pK_a ∼ 9.5 from the different values reported), 75-fold lower than the cysteine thiolate (pK_a ∼ 7.5).[3] The lower k_2 reflects a combination of stereoelectronic effects: a larger ring size in the transition state (6 versus 5), as well as the higher pK_a of the γ-thiol converts the thiolate into a poorer leaving group.

The NCL between **1** (1.4 mM) and **11** (5.2 mM) displayed a different kinetic profile from those of **2** and **7** (Figures 5a,c). First, a large initial buildup of the intermediate (**12**, 86% of the total product), and then its slow disappearance to give the final peptide **13**. The high concentration of **12** controls the reaction rate, and determines the second step as the rate-limiting as similarly observed with other N-auxiliaries.[16−19] Rate constant calculations resulted in (Table 1, entry 5): k_1 = (5.5 ± 0.4) $M^{-1}s^{-1}$ and k_2 = (0.0012 ± 0.0002) s^{-1} ($t_{1/2}$ = 577 s). That represents a 1.7-fold faster first step, but a 13-fold slower second reaction. The difference in k_1 compared to the NCL with **2** could be derived from subtle changes in the pK_a of the thiol. However, the steric hindrance of the methyl group rules the rearrangement rate by reducing 1 order of magnitude the k_2 constant. This effect is even more noticeable in the ligation with (MehCys)TAFS: after 95 h of reaction, 31% of the unrearranged product was still present (Figure S57).

NCL between CTAFS and C-Terminal Ala-SePh and Pro-SePh

Next, we focused our study on the ligation with other representative C-terminal residues such as Ala and Pro (Scheme 3). Ala is α-substituted, and less hindered than Val. Previous results have shown a kinetics similar to Gly and His, but slightly

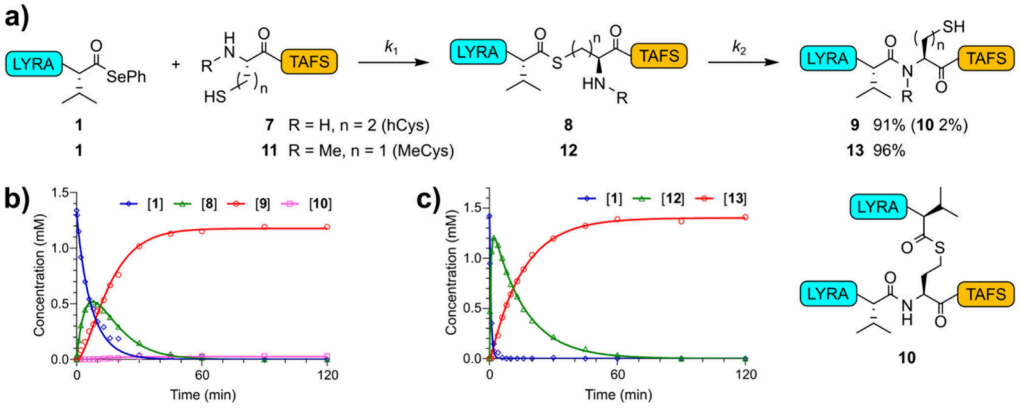

Figure 5. (a) NCL between peptides **1** and **7**, **1** and **11**; experimental data (dots) and their corresponding curve fitting (solid lines) using the model **1** + **7** → **8** → **9** + **1** → **10** (b) and **1** + **11** → **12** → **13** (c).

https://doi.org/10.1021/jacsau.4c00705
JACS Au 2024, 4, 4374−4382

Scheme 3. NCL between Peptides 2 and 14 or 18

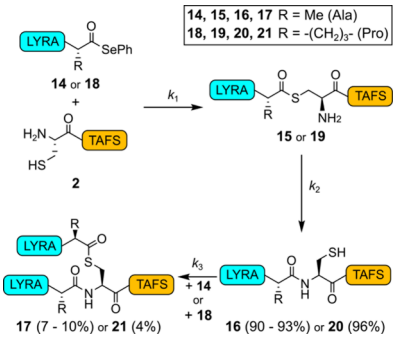

faster compared to Leu and Tyr.[7,9] NCL between LYRAA-COSePh (**14**, 0.80−1.2 mM) and **2** (2.6−2.8 mM) led to a completion of the reaction in 2 min (Figures S59, S61, and S62). Although under these conditions it was very challenging to observe **AB** (**15**) due to the fast reaction time and low accumulation, we could measure a k_{obs} (k_{12}) = (26 ± 6) $M^{-1}s^{-1}$ (Table S10). The use of a larger excess of **2** (8.3 mM) and a $[\mathbf{14}]_O$ = 0.90 − 1.3 mM, allowed the visualization of **15** and measurement of both k_1 = (26 ± 2) $M^{-1}s^{-1}$ and k_2 = (0.22 ± 0.01) s^{-1} ($t_{1/2}$ = 3 s) (Table 1, entry 8 and Figures S63, S65, and S66). Other α-substituted amino acids should have rate constant values between those of Ala and Val, or slightly faster for residues where the electron-withdrawing character is higher, like His. Interestingly, the ligation between **14** and (MehCys)TAFS led to the complete rearranged amide product (k_2 ∼ 0.0003 s^{-1}, $t_{1/2}$ ∼ 39 min) confirming the major influence of the steric effects in the *S-to-N* acyl shift (Figures S67 and S69).

Pro is one of the most intriguing amino acids. NCL at the C-terminal Pro-α-thioester gives the slowest reaction rate. Experimental and theoretical studies suggest an n → π^* interaction between the carbonyl orbitals of Pro and the adjacent residue as the main factor of the decreased electrophilicity.[30,31] The ligations between LYRAP-COSePh (**18**) and **2** gave a k_1 = (0.72 ± 0.03) $M^{-1}s^{-1}$ and a k_2 = (0.031 ± 0.001) s^{-1} ($t_{1/2}$ = 22 s), (Table 1, entry 9 and Figures S70, S72, and S73). As expected, the intermolecular reaction is slower, and likely rate-limiting. At a $[\mathbf{18}]_o$ = 1.5 mM, it would be necessary a 16-fold excess to invert and make the first step faster. The 7-fold lower k_2 compared to Ala points to the constraint imposed by the Pro side chain ring in the transition state. However, the electronic parameters affect less the rearrangement because this value is almost 2-fold higher than in Val (compare the k_1 for Val = 3.2 versus Pro = 0.72).

To test the n → π^* hypothesis we prepared a peptide with a more electrophilic carbonyl at Pro and a thiol-leaving group poorer than phenylselenol: LYRAP(4,4-difluoro)-COS(4-MPOH).[25] The ligation of this peptide with **2** achieved completion around 4 h (Figure S75). These experiments confirm the main contribution of electronic factors to the decreased reactivity of Pro.

Implications of the NCL Mechanism

Several implications of the NCL mechanism can be inferred:

1. Under standard NCL conditions, the thiol-thioester exchange is the rate-limiting step (Scheme 1, step 1). Considering that phenyl α-thioesters have, at least, second-order rate constants 1 order of magnitude lower than phenyl α-selenoesters, then the accumulation of the intermediate α-thioester **AB** is very small (almost untraceable by analytical HPLC). In this situation, **AB** can be ignored and the model is simplified as a one-step bimolecular reaction: **A** + **B** → **P**.
2. The steric impediment of the C-terminal residue and the N-terminal auxiliaries in **A** and **B** peptides, respectively, governs the rearrangement rate.
3. Phenyl α-selenoesters react faster than phenyl α-thioesters. However, the difference in pK_a for phenylselenol and 4-MBA (∼4.6 versus 5.5, respectively) cannot draw definitive conclusions. It is necessary to contrast the reactivity with phenyl α-thioesters having a thiol-leaving group with similar pK_a, such as 4-nitrothiophenol or 5-thio-2-nitrobenzoic acid.
4. The use of highly activated phenyl α-selenoesters has important advantages over thioesters. Mainly, faster rates resulting from a larger k_1 permit the use of lower concentrations of reactants, particularly useful in the case of aggregating peptides or NCL with large protein segments. Nevertheless, it always becomes indispensable to use more than 2 equivalents of peptide **B** because of the competing reactions, principally branched peptides and hydrolysis. Alternatively, NCL at acidic pH ∼ 5 using N-terminal selenocysteine is likely a more appealing strategy.[24]
5. The k_1 values reported here reflect the initial total concentration of the **B** peptide, but not the thiolate-reacting peptide. Those rate constants are higher, particularly in the case of hCys thiolate.[32]
6. Lastly, the pH and other reaction conditions can affect the rates of both steps. For instance, if NCL is carried out under folding conditions,[33] in templated ligations,[22] or in expressed protein ligation.[34] In these scenarios, conformational constraints could be involved.

CONCLUSIONS

In summary, the elusive transient thioester of the NCL was observed and characterized under standard ligation conditions. The key element of this finding was the fast acceleration of the intermolecular thiol-selenoester exchange allowing the accumulation of the intermediate. The *S-to-N* acyl shift rate strongly depends on the nature of the intermediate α-thioester residue, resulting in a difference of 1 order of magnitude between Ala and Val. Its contribution to the reaction rate is important in Val, and likely in other residues bearing bulky side chains.

Future work with phenyl α-selenoester peptides will investigate what step is rate-limiting, and if the thiol-(α-selenoester) exchange (step 1) proceeds via a tetrahedral intermediate or a concerted asynchronous mechanism. Regarding these questions, DFT calculations of the free energies of activation using simple NCL models (formyl-Gly-SPh + Cys) point out a difference of only 1.1 kcal.mol^{-1} between the transition state of step 1 (higher energy) and the highest energy transition state of step 2.[35] In addition, this study shows that a one-step direct attack of the Cys thiolate and displacement of thiophenol via an asymmetric reaction coordinate profile is energetically more preferred than a proposed addition−elimination mechanism. Because phenyl α-selenoesters are energetically richer than phenyl α-thioesters, both a change in the rate-determining step and step 1 via a S_N2 pathway are conceivable.

https://doi.org/10.1021/jacsau.4c00705
JACS Au 2024, 4, 4374−4382

METHODS

Synthesis of Peptides CTAFS, (hCys)TAFS, (MeCys)TAFS, (MehCys)TAFS, LYRAVCTAFS, and LYRAV*CTAFS

Peptide synthesis (Rink-Amide Aminomethyl resin, 0.2 mmol scale) was carried out using standard Fmoc-SPPS protocols. Coupling: Fmoc-aa (1.0 mmol) preactivated for 3 min with 1-*tert*-Butyl-3-ethyl-carbodiimide (T-BEC, 1.0 mmol) and 5-(hydroxyimino)-1,3-dimethylpyrimidine-4,4,6(1*H*,3*H*,5*H*)-trione (Oxy-B, 1.0 mmol). Following the addition of the mixture to the peptidyl-resin, DIEA (0.5 mmol) was added. The coupling time was 45 min. Fmoc removal: 20% piperidine/DMF (2 × 1 min, 1 × 5 min). Cleavage: TFA:H_2O:TIS (95:2.5:2.5, 10 mL/1 g peptidyl-resin, 90 min). Workup: the TFA was removed to a minimal volume by evaporation under a N_2 stream. Cold Et_2O was added, and the resulting precipitate was centrifuged. The supernatant was discarded, and the pellet dried under a N_2 stream. Next, the solid was dissolved in H_2O/ACN (1:1) and freeze-dried. The crude peptides were purified by semipreparative HPLC (Waters). The pure fractions were pooled together, and freeze-dried. Peptide purity was analyzed by analytical HPLC (Agilent 1100 series) using a C18 reverse-phase column hyphenated to a photodiode array detector. Runs were simultaneously monitored at 220 and 280 nm. Mass analysis was performed on a MALDI-TOF (Bruker Daltonics).

Synthesis of α-Thioester and α-Selenoester Peptides: LYRAXaa-COSePh (Xaa = A, V, V*, P), LYRAV-COS(4-MBA), and LYRAP(4,4-difluoro)-COS(4-MPOH)

Synthesis of the phenyl α-thioester and phenyl α-selenoester sequences was carried out using LYRAXaa-CODbz (Dbz = *o*-aminoanilide) peptides prepared following reported procedures.[25] Briefly, in a plastic tube (15 mL), the crude LYRAXaa-CODbz peptide (100 mg) was dissolved in DMF (1.8 mL) and AcOH (0.2 mL). The mixture was cooled in an ice bath for 5 min. Then, ^{t}BuONO (0.2 mL) was added, and the resulting mixture was kept in the ice with periodic shaking. Complete Dbz to benzotriazole oxidation was achieved in 30 min. Next, cold Et_2O (12 mL) was added, and the mixture spun out. The supernatant was discarded and the pellet was dried under a N_2 stream.

For Phenyl α-Selenoesterification. DPDS (100 mg, 0.320 mmol) and TCEP.HCl (168 mg, 0.586 mmol) were dissolved in degassed phosphate buffer (6 M Gdm, 0.2 M sodium phosphate, 3.0 mL, pH of the mixture adjusted to 7.5) under sonication. Then, the pH was fitted to 7.0 using $HCl_{(aq)}$ (1 M), and the resulting solution was added to the peptide pellet (the final pH of the reaction was 6.6). The mixture was stirred at 23 °C until complete exchange (5 min for Ala, 45 min for Val and Pro). The crude reaction mixture was directly purified by semipreparative HPLC. The pure fractions were combined and lyophilized. Yields: 25 − 45%.

For Phenyl α-Thioesterification. 4-MBA (30.8 mg, 0.20 mmol) or 4-MPOH (25.2 mg, 0.20 mmol), and TCEP.HCl (22.9 mg, 0.0810 mmol) were dissolved in degassed phosphate buffer (6 M Gdm, 0.2 M sodium phosphate, 2.0 mL, pH = 6.6). This solution was added to the peptide pellet, and the mixture was stirred at 23 °C for 30 min. Next, the solution was acidified with $HCl_{(aq)}$ (1 M) until pH = 2.0, and the 4-MBA or 4-MPOH were removed through Et_2O extraction (2 × 5 mL). The resulting aqueous solution containing the peptide was purified by semipreparative HPLC. The pure fractions were combined and lyophilized. Yields: 40 − 60%.

^{1}H NMR and ^{13}C NMR

^{1}H NMR experiments were registered in a Bruker Ascend (9.4 T, 400 MHz for ^{1}H) equipped with a room temperature iProbe. For the determination of the net peptide content, known amounts of sodium acetate (Fluka 98.5%, internal standard reference) and peptide were dissolved in D_2O (0.7 mL).[36] DCl (1 mM) was added for thioester and selenoester peptides. The experiments were recorded using a d_1 = 30 s, and a spectral window = 15-(−5) ppm. Sixteen scans were accumulated for a total acquisition time of 12.5 min. Analysis of the spectra was performed with Bruker TopSpin 4.4.0. The integrated areas of the different peptide ^{1}H nuclei and acetate were used to calculate the net peptide content: **1** (68.0%), **2** (82.5%), **4*** (73.0%, the same percentage was used for **4**, **3**, and **3***), **6** (71.5%), **7** (81.0%), **11** (80.0%), **14** (52.0%), **18** (68.6%).

^{13}C NMR of peptides **3*** and **4*** was registered on a Bruker AVANCEIIIHD (11.7 T, 126 MHz for ^{13}C) equipped with a TCI Cryoprobe. Peptides (2.20 mg) were dissolved in D_2O/CH_3CN (9:1, 0.6 mL) containing DCl (5.0 mM). The experiments were recorded at 298 K using a d_1 = 2 s, and a spectral window = 230-(−20) ppm. 8783 scans were accumulated for a total acquisition time of 16 h.

NCL with Model Peptides

For kinetic experiments, peptide samples were weighed in a Mettler Toledo XPR2U microbalance (accuracy of ± 0.001 mg). All the other reagents were weighed in a Sartorius CP225D balance (accuracy of ± 0.01 mg). pH measurements were performed using a sensiON pH31 (accuracy ± 0.01) equipped with a Hach 52 09 probe, and a Crison (model 506, accuracy ± 0.01) with a Hach 52 08 probe. Both probes were used to double-check the pH of the ligations.

All reactions were carried out at 23 °C under N_2 atmosphere. First, stock solutions of H-Tyr-OH (20.0 mM in H_2O) and phosphate buffer (6 M Gdm.HCl, 0.2 M sodium phosphate, pH = 7.3) were degassed by passing through a N_2 stream for 15 min. These stocks were used to prepare the ligation buffer containing the desired concentrations of TCEP, DPDS/4-MBA/4-MPOH, and Tyr (2.0 mM). Ascorbic acid (0.2 M) was added when the desulfurization was observed in preliminary experiments.[37] pH adjustments were performed using stock solutions of $NaOH_{(aq)}$ (10 and 1 M) and $HCl_{(aq)}$ (6 and 1 M).

In a typical experiment, the acceptor peptide **B** was dissolved in the ligation buffer (0.60 mL, pH of the mixture 7.0 − 7.10) and then added to the donor peptide **A**. The pH of the reaction was measured at the end of the ligation, resulting always in the range of 6.9 − 7.0. Aliquots of 20 μL were withdrawn at the selected times and quenched with a solution of HCl (0.5 M, 8:2 H_2O/CH_3CN, 20 μL). The reaction vial was flushed with N_2 every time after each aliquot was removed (except for the ligation with LYRAA-COSePh). The quenched samples were spun out to discard any precipitate, and the supernatant (5 μL) was analyzed by HPLC the same day. Injections were simultaneously monitored at 220 and 280 nm. Compounds corresponding to the different HPLC peaks of the ligation were collected and analyzed by MALDI-TOF mass spectrometry.

AB, **P**, **PA**, and $\mathbf{A_{OH}}$ (hydrolyzed α-selenoester/thioester peptide, if any) concentrations were determined experimentally by integrating the corresponding HPLC peak areas at 280 nm (Tyr absorption) and referenced to the Tyr area ([Tyr] = 2.0 mM, internal standard).

$$[\mathbf{AB/P/A_{OH}}] = \frac{\text{Area}_{280\text{nm}\mathbf{AB/P/AOH}} \times 2.0\ \text{mM}}{\text{Area}_{280\text{nmTyr}}}$$

$$[\mathbf{PA}] = \frac{\text{Area}_{280\text{nm}\mathbf{PA}} \times 2.0\ \text{mM}}{2 \times \text{Area}_{280\text{nmTyr}}}$$

Peptide **A** concentrations were estimated from a mass balance:

$$[\mathbf{A}]_o = [\mathbf{P}]_{final} + [\mathbf{AB}]_{final} + [\mathbf{A_{OH}}]_{final} + 2[\mathbf{PA}]_{final}$$

$$[\mathbf{A}]_t = [\mathbf{A}]_o - ([\mathbf{P}]_t + [\mathbf{AB}]_t + [\mathbf{A_{OH}}]_t + 2[\mathbf{PA}]_t)$$

Kinetic Modeling and Calculation of the Rate Constants

For the calculation of the kinetic parameters, three independent replicates for each reaction were carried out. The initial concentrations of peptides $\mathbf{A/A_{Se}}$ and **B** varied in each replicate.[38] Full reaction profiles of **AB**, **P**, **PA**, and $\mathbf{A_{OH}}$ (only when detected in the ligation) were analyzed. Model simulations and rate constant calculations were performed in COPASI (4.37 and 4.42) using equations describing elementary reaction steps. The theoretical kinetic model included the following terms (Scheme 4):

- A second-order bimolecular reaction: $\mathbf{A/A_{Se}} + \mathbf{B} \rightarrow \mathbf{AB}$ (**AB** formation, k_1)
- A first-order unimolecular reaction: $\mathbf{AB} \rightarrow \mathbf{P}$ (**P** formation, k_2)
- A second-order bimolecular reversible reaction: $\mathbf{A/A_{Se}} + \mathbf{P} \rightleftharpoons \mathbf{PA} + \mathbf{RSH/RSeH}$ (**A**, **P**, branched thioester **PA** and phenylselenol/4-MBA equilibrium, k_3 and k_{-3})

https://doi.org/10.1021/jacsau.4c00705
JACS Au 2024, 4, 4374−4382

Scheme 4. Kinetic Model and Rate Equations

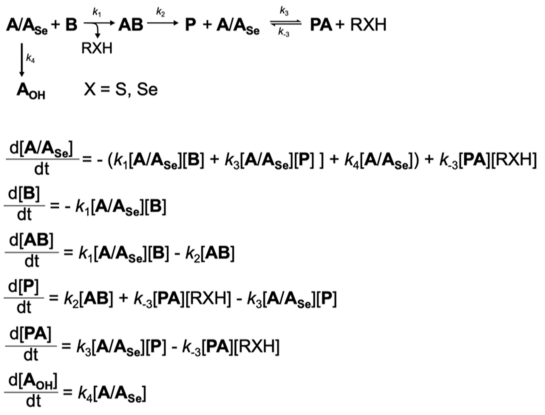

- A pseudo-first-order unimolecular reaction: **A**/**A**$_{Se}$ → **A**$_{OH}$ (**A**/**A**$_{Se}$ hydrolysis, k_4, only when observed)

The formation of the branched product **PA** under phenylselenol conditions can be treated as irreversible ($k_3 \gg k_{-3}$). Thus, the term k_{-3}[PA][RSeH] ∼ 0. However, under phenyl thiol conditions, the backward reaction (k_{-3}) is significant, and the equilibrium is determined by the ratio of the constants k_3/k_{-3}. The hydrolysis term (k_4) was included when the hydrolyzed α-selenoester/thioester peptide was detected to keep the mass balance, and not overestimate k_1.

The experimental concentrations of **AB**, **P**, **PA**, **A**$_{OH}$ (if any), and [**B**]$_o$ (reactant in excess) were introduced in COPASI. According to the theoretical kinetic model, the corresponding k_i were estimated by applying a Differential Evolution algorithm.[39] The system was iterated until the k_i remained significantly unchanged and the fitted values had a root-mean-square < 5 × 10^{-6}. Each replicate was modeled separately. The calculated parameters were validated by plotting the experimental and the fitting data. The calculated k_i values are expressed as the average ± standard deviation. Data obtained from the experiments and the simulations were plotted using GraphPad Prism 8.

■ ASSOCIATED CONTENT

Supporting Information

The Supporting Information is available free of charge at https://pubs.acs.org/doi/10.1021/jacsau.4c00705.

Detailed experimental procedures for ligation reactions; MALDI-TOF mass spectrometry; ^{1}H NMR and ^{13}C NMR spectra; HPLC traces of the reactions; curve fitting of the experimental data and calculation of the kinetic constants (PDF)

■ AUTHOR INFORMATION

Corresponding Author

Juan B. Blanco-Canosa − *Institute for Advanced Chemistry of Catalonia (IQAC), Spanish National Research Council (CSIC), 08034 Barcelona, Spain;* orcid.org/0000-0001-5738-6993; Email: juanbautista.blanco@iqac.csic.es

Author

Iván Sánchez-Campillo − *Institute for Advanced Chemistry of Catalonia (IQAC), Spanish National Research Council (CSIC), 08034 Barcelona, Spain; Department of Inorganic and Organic Chemistry, Section of Organic Chemistry, University of Barcelona, 08028 Barcelona, Spain;* orcid.org/0000-0002-8666-8065

Complete contact information is available at: https://pubs.acs.org/10.1021/jacsau.4c00705

Author Contributions

I. S.-C. and J. B. B. C. performed peptide synthesis, NMR analysis, MALDI-TOF mass spectrometry, NCL with model peptides, model simulations, and k_i calculations, analyzed and interpreted the data, and participated in the manuscript preparation. J. B. B. C. devised the original idea. I. S.-C. and J. B. B. C. contributed with new ideas. J. B. B. C. wrote the first draft of the paper with contributions from I. S.-C. J. B. B. C. supervised the project. I. S.-C. and J. B. B. C. approved the final version of the manuscript. CRediT: I. S.-C.: methodology, validation, formal analysis, investigation, resources, data curation, visualization, writing − review and editing; J. B. B. C.: conceptualization, methodology, validation, formal analysis, investigation, resources, data curation, visualization, supervision, project administration, funding acquisition, writing − original draft, writing − review and editing.

Funding

This work has been funded by the Spanish Ministerio de Ciencia, Innovación y Universidades (PDI2021-128902OB-I00). I. S.-C. acknowledges AGAUR (Generalitat de Catalunya) for a fellowship (2021 FI-B 00142).

Notes

The authors declare no competing financial interest.

■ ACKNOWLEDGMENTS

We acknowledge Sonia Pérez (IQAC) for the use of the ultramicrobalance, and Luxembourg Bio Technologies for generously supplying T-BEC and Oxy-B.

■ REFERENCES

(1) Dawson, P. E.; Muir, T. W.; Clark-Lewis, I.; Kent, S. B. H. Synthesis of proteins by native chemical ligation. *Science* **1994**, *266*, 776−779.

(2) Dawson, P. E.; Kent, S. B. H. Synthesis of proteins by chemical ligation. *Annu. Rev. Biochem.* **2000**, *69*, 923−960.

(3) Agouridas, V.; El Mahdi, O.; Diemer, V.; Cargoët, M.; Monbaliu, J.-C. M.; Melnyk, O. Native chemical ligation and extended methods: mechanisms, catalysis, scope, and limitations. *Chem. Rev.* **2019**, *119* (12), 7328−7443.

(4) Conibear, A. C.; Watson, E. E.; Payne, R. J.; Becker, C. F. W. Native chemical ligation in protein synthesis and semi-synthesis. *Chem. Soc. Rev.* **2018**, *47*, 9046−9068.

(5) Wieland, T.; Bokelmann, E.; Bauer, L.; Lang, H. U.; Lau, H. Über Peptidsynthesen. 8. Mitteilung Bildung von S-Haltigen Peptiden Durch Intramolekulare Wanderung von Aminoacylresten. *J. Liebigs Ann. Chem.* **1953**, *583*, 129−148.

(6) Kent, S. B. H. Total chemical synthesis of proteins. *Chem. Soc. Rev.* **2009**, *38*, 338−351.

(7) Hackeng, T. M.; Griffin, J. H.; Dawson, P. E. Protein synthesis by native chemical ligation: expanded scope by using straightforward methodology. *Proc. Natl. Acad. Sci. USA* **1999**, *96*, 10068−10073.

(8) Dawson, P. E.; Churchill, M. J.; Ghadiri, M. R.; Kent, S. B. H. Modulation of reactivity in native chemical ligation through the use of thiol additives. *J. Am. Chem. Soc.* **1997**, *119* (19), 4325−4329.

(9) Johnson, E. C. B; Kent, S. B. H. Insights into the mechanism and catalysis of the native chemical ligation reaction. *J. Am. Chem. Soc.* **2006**, *128* (20), 6640−6646.

(10) Mende, F.; Seitz, O. 9-Fluorenylmethoxycarbonyl-based solid-phase synthesis of peptide α-thioesters. *Angew. Chem., Int. Ed.* **2011**, *50*, 1232−1240.

(11) Yan, L. Z.; Dawson, P. E. Synthesis of peptides and proteins without cysteine residues by native chemical ligation combined with desulfurization. *J. Am. Chem. Soc.* **2001**, *123* (4), 526−533.

(12) Gieselman, M. D.; Xie, L.; Van Der Donk, W. A. Synthesis of a selenocysteine-containing peptide by native chemical ligation. *Org. Lett.* **2001**, *3* (9), 1331−1334.
(13) Hondal, R. J.; Nilsson, B. L.; Raines, R. T. Selenocysteine in native chemical ligation and expressed protein ligation. *J. Am. Chem. Soc.* **2001**, *123* (21), 5140−5141.
(14) Wan, Q.; Danishefsky, S. J. Free-radical-based, specific desulfurization of cysteine: a powerful advance in the synthesis of polypeptides and glycopeptides. *Angew. Chem., Int. Ed.* **2007**, *46*, 9248−9252.
(15) Metanis, N.; Keinan, E.; Dawson, P. E. Traceless ligation of cysteine peptides using selective deselenization. *Angew. Chem., Int. Ed.* **2010**, *49*, 7049−7053.
(16) Canne, L. E.; Bark, S. J.; Kent, S. B. H. Extending the applicability of native chemical ligation. *J. Am. Chem. Soc.* **1996**, *118* (25), 5891−5896.
(17) Offer, J.; Boddy, C. N.; Dawson, P. E. Extending synthetic access to proteins with a removable acyl transfer auxiliary. *J. Am. Chem. Soc.* **2002**, *124* (17), 4642−4646.
(18) Offer, J. Native chemical ligation with N^{α} acyl transfer auxiliaries. *Pept. Sci.* **2010**, *94* (4), 530−541.
(19) Loibl, S. F.; Harpaz, Z.; Seitz, O. A type of auxiliary for native chemical ligation beyond cysteine and glycine junctions. *Angew. Chem., Int. Ed.* **2015**, *54*, 15055−15059.
(20) Bondalapati, S.; Jbara, M.; Brik, A. Expanding the chemical toolbox for the synthesis of large and uniquely modified proteins. *Nat. Chem.* **2016**, *8*, 407−418.
(21) Kulkarni, S. S.; Sayers, J.; Premdjee, B.; Payne, R. J. Rapid and efficient protein synthesis through expansion of the native chemical ligation concept. *Nat. Rev. Chem.* **2018**, *2*, 0122.
(22) Severin, K.; Lee, D. H.; Kennan, A. J.; Ghadiri, M. R. A synthetic peptide ligase. *Nature* **1997**, *389*, 706−709.
(23) Durek, T.; Alewood, P. F. Preformed selenoesters enable rapid native chemical ligation at intractable sites. *Angew. Chem., Int. Ed.* **2011**, *50*, 12042−12045.
(24) Mitchell, N. J.; Malins, L. R.; Liu, X.; Thompson, R. E.; Chan, B.; Radom, L.; Payne, R. J. Rapid additive-free selenocystine-selenoester peptide ligation. *J. Am. Chem. Soc.* **2015**, *137* (44), 14011−14014.
(25) Sánchez-Campillo, I.; Miguel-Gracia, J.; Karamanis, P.; Blanco-Canosa, J. B. A versatile *o*-aminoanilide linker for native chemical ligation. *Chem. Sci.* **2022**, *13*, 10904−10913.
(26) Hoops, S.; Sahle, S.; Gauges, R.; Lee, C.; Pahle, J.; Simus, N.; Singhal, M.; Xu, L.; Mendes, P.; Kummer, U. COPASI-a COmplex PAthway SImulator. *Bioinformatics* **2006**, *22* (24), 3067−3074.
(27) Eldin, S.; Jencks, W. P. Lifetimes of iminium ions in aqueous solution. *J. Am. Chem. Soc.* **1995**, *117* (17), 4851−4857.
(28) Tam, J. P.; Yu, Q. Methionine ligation strategy in the biomimetic synthesis of parathyroid hormones. *Biopolymers* **1998**, *46* (5), 319−327.
(29) Tanaka, T.; Wagner, A. M.; Warner, J. B.; Wang, Y. J.; Petersson, E. J. Expressed protein ligation at methionine: N-terminal attachment of homocysteine, ligation, and masking. *Angew. Chem., Int. Ed.* **2013**, *52*, 6210−6213.
(30) Pollock, S. B.; Kent, S. B. H. An investigation into the origin of the dramatically reduced reactivity of peptide-prolyl-thioesters in native chemical ligation. *Chem. Commun.* **2011**, *47*, 2342−2344.
(31) Hinderaker, M. T.; Raines, R. T. An electronic effect on protein structure. *Protein Sci.* **2003**, *12* (6), 1188−1194.
(32) Maguire, O. R.; Zhu, J.; Brittain, W.D. G.; Hudson, A. S.; Cobb, S. L.; O'Donoghue, A. C. N-terminal speciation for native chemical ligation. *Chem. Commun.* **2020**, *56*, 6114−6117.
(33) Beligere, G. S.; Dawson, P. E. Conformationally assisted protein ligation using C-terminal thioester peptides. *J. Am. Chem. Soc.* **1999**, *121* (26), 6332−6333.
(34) Muir, T. W.; Sondhi, D.; Cole, P. A. Expressed protein ligation: a general method for protein engineering. *Proc. Natl. Acad. Sci. USA* **1998**, *95* (12), 6705−6710.
(35) Wang, C.; Guo, Q.-X.; Fu, Y. Theoretical analysis of the detailed mechanism of native chemical ligation reactions. *Chem.-Asian J.* **2011**, *6*, 1241−1251.
(36) Rundlöf, T.; Mathiasson, M.; Bekiroglu, S.; Hakkarainen, B.; Bowden, T.; Arvidsson, T. Survey and qualification of internal standards for quantification by ^{1}H NMR spectroscopy. *J. Pharm. Biomed. Anal.* **2010**, *52*, 645−651.
(37) Dardashti, R. N.; Metanis, N. Revisiting ligation at selenomethionine: Insights into native chemical ligation at selenocysteine and homoselenocysteine. *Bioorg. Med. Chem.* **2017**, *25*, 4983−4989.
(38) Jencks, W. P. *Catalysis in Chemistry and Enzymology*; McGraw-Hill Book Company: New York, 1969; p 556.
(39) Storn, R.; Price, K. Differential Evolution - A Simple and Efficient Heuristic for global Optimization over Continuous Spaces. *Journal of Global Optimization* **1997**, *11*, 341−359.

https://doi.org/10.1021/jacsau.4c00705
JACS Au 2024, 4, 4374−4382